On the Comparative Analysis of the Band Structure of One-Dimensional Photonic Crystal with Different Material Composition under Oblique Wave Incidence

Arpan Deyasi[1], Sourangsu Banerji[2]
[1]deyasi_arpan@yahoo.co.in; [2]sourangsu.banerji@gmail.com

Abstract

In this paper, band structure of one dimensional photonic crystal is studied for different material compositions under oblique incidence of electromagnetic wave. Computation is carried out for both SiO_2/Air and $Al_xGa_{1-x}N$/GaN compositions. Comparative analysis shows the superiority of the semiconductor heterostructure based photonic crystal structure over the conventional system. The study proves the dominance of semiconductor heterostructure based fabrication which can be put to effective use in the manufacture of photonic crystal based devices.

Keywords

Photonic crystals, Photonic bandgap, semiconductor heterostructure, Band structure

Introduction

Photonic crystal is a periodic arrangement of dielectric materials [1] where the localization of electromagnetic wave propagating inside is controlled by suitably varying the structural parameters. Because of the periodicity, the structure exhibits windows in otherwise prohibited wavelength spectra mainly due to the formation of photonic bandgap, which may be exhibited in any one, two or three dimensions [1-2]. This property is mainly responsible to block the propagation of some wavelength, and allows other wavelength in the spectra; and thus can effectively be considered as an optical bandpass filter [3]. This phenomenon can be explained by the principle of Bragg's reflection [4], where we assume that wavelength of light will be of the order of layer dimensions [5]. Materials exhibiting photonic bandgap can be used in designing photonic crystal fiber [6], which may replace the conventional optical fiber due to its highly improved performance from communication point-of-view [7]. It is used to construct optical transmitter [8], switch [9], waveguide [10] etc.

Band structure is one of the most important concepts in solid state physics as well as in photonics, the knowledge of which helps to determine the dispersion relation of infinitely extended defect free photonic crystals. Bandgap of two dimensional photonic crystals had previously been studied by varying column roundness by Hillebrand [11] using plane-wave expansion method. Recently, finite-difference-time-domain method was used to analyze the forbidden region of photonic crystal with different geometries [12]. Zhao calculated the width of bandgap [13] using Bragg's principle of reflection. Men optimized the computational problem using semi-definite programming and subspace methods [14]. Evolutionary algorithm [15] and level-set method [16] have also been used for design of large bandgap crystal. In the present paper, band structure of

one-dimensional photonic crystal is calculated by using plane wave expansion method technique, and AlGaN/GaN material composition is considered as a unit cell of the periodic arrangement. The use of semiconductor heterostructure adds novelty of the work in the respect that the structure can be treated as photonic multiple quantum well for electronic applications [17], and also it provides better performance as optical transmitting/emitting device [18]. This structure can also be embedded in the active region of VCSEL, which adds tunability of its filter characteristics [19]. Use of AlGaN/GaN material composition is taken up because as shown in [20], the predominant effect of carrier localization in undoped AlGaN alloys enhances with the increase in Al contents and is related to the insulating nature of AlGaN of high Al contents. Usage of high Al-content AlGaN layer also increases the overall figure of merit of the AlGaN/GaN due to the combined advantages of enhanced band offset, lattice mismatch induced piezoelectric effect. The advantages of GaN can be summarized as ruggedness, power handling and low loss [21], [22].

In the current paper, detailed analytical study of the photonic band structure has been out for different material compositions under oblique wave incidence. Oblique wave incidence which is characterized by both the TE (Transverse Electric) and TM (Transverse Magnetic) mode i.e. both s and p polarization help us to understand the photonic band structure pointing out the advantage of the use of semiconductor heterostructure based fabrication in photonic devices in comparison to the traditional material composition .The comparative, matched results along with the detailed analysis bore testimony to the previous statement.

Mathematical Modeling

Lying on the fundamental principles of the Bloch function and the Fourier transform, the plane wave method (PWM) applies to a periodic structure of a photonic crystal in the wave vector-space. On solving the Maxwell equations, eigen-values can be obtained to extract the dispersive feature of the photonic energy band. So much so, that by using the approximation of linear and lossless material, Maxwell equations can be written as:

$$\nabla.D(r,t) = 0 \tag{1}$$

$$\nabla.B(r,t) = 0 \tag{2}$$

$$\nabla \times H(r,t) = \frac{\partial D(r,t)}{\partial t} \tag{3}$$

$$\nabla \times E(r,t) = -\frac{\partial B(r,t)}{\partial t} \tag{4}$$

where the terms D, B, E, and H are the displacement, magnetic, electrical, and inductive fields of an electromagnetic wave propagating in the photonic crystal respectively, On the Assumption that both E(r, t) and H(r, t) have sine surge modes with respect to real space r and time t, then Maxwell equations can be written as:

$$\nabla.\varepsilon(r).E(r) = 0 \tag{5}$$

$$\nabla.B(r,t) = 0 \tag{6}$$

$$\nabla \times H(r) = i\omega\varepsilon_0\varepsilon(r)E(r) \tag{7}$$

$$\nabla \times E(r) = -i\omega\mu_0 H(r) \tag{8}$$

where ω is the oscillation frequency of the electromagnetic field, ε(r) is the corresponding dielectric constant of the crystal and is a function of space r, also ε_0 and μ_0 denote the dielectric constant and permeability in vacuum, respectively. On mathematically solving these equations in addition to the consideration of the harmonic mode, a simple important equation obtained can be written as:

$$\nabla \times \frac{1}{\varepsilon(r)} \nabla \times \vec{H}(r) = \frac{\omega^2}{C^2} \vec{H}(r) \tag{9}$$

Using Bloch's theorem, essentially in the case of an infinite periodic photonic crystal, a mode in a periodic structure can be expressed as a sum of infinite number of plane waves:

$$H(r) = \sum_{\vec{G}_i, \lambda} h_{G_i, \lambda} e^{i(\vec{k}+\vec{G}_i).\vec{r}} \hat{e}_\lambda \tag{10}$$

where λ=1, 2, also k denotes the wave vector of the plane wave, $\vec{G}$ is the reciprocal lattice vector , $\hat{e}_\lambda$ is used to denote the two unit axis perpendicular to the propagation direction $\vec{k} + \vec{G}$. $h_{G_i, \lambda}$ is used to represent the coefficient of the H component along the axes $\hat{e}_\lambda$. One thing to note here is that ($\hat{e}_1$, $\hat{e}_2$, $\vec{k} + \vec{G}$) are perpendicular to each other.

Now, using the Fourier transform, the dielectric function can also be written as,

$$\varepsilon(r) = \sum_{\vec{G}} \varepsilon(\vec{G}) \exp(i\vec{G}.r) \tag{11}$$

$$\varepsilon(\vec{G}) = \frac{1}{V} \iiint_{\Omega} \varepsilon(r) \exp(-i\vec{G}.r) \tag{12}$$

where Ω is the unit cell and V is the volume of the unit cell.

Eventually, Helmholtz's equation can be expressed in a form which is standard eigen-value problem,

$$\sum_{\vec{G}'} |k+G\|k+G'|\varepsilon^{-1}(G-G') \begin{bmatrix} \hat{e}_2\hat{e}_2' & -\hat{e}_2\hat{e}_1' \\ -\hat{e}_1\hat{e}_2' & \hat{e}_1\hat{e}_1' \end{bmatrix} \begin{bmatrix} h_1' \\ h_2' \end{bmatrix} = \frac{\omega^2}{C^2} \begin{bmatrix} h_1 \\ h_2 \end{bmatrix} \tag{13}$$

Here, $\begin{bmatrix} \hat{e}_2\hat{e}_2' & -\hat{e}_2\hat{e}_1' \\ -\hat{e}_1\hat{e}_2' & \hat{e}_1\hat{e}_1' \end{bmatrix}$ matrix gives us the direction of the wave vector propagation when it strikes a lattice site; i.e. causes diffraction on hitting a Bragg plane in the first Brillouin zone. Certain simplifications exist for both 1D and 2D case as well as for both in-plane and off-plane light propagation. $\begin{bmatrix} h_1' \\ h_2' \end{bmatrix}$ is an NX1 matrix which satisfies the number of plane waves that is being considered. Coming to the one dimensional normal incidence case, here both the TE and TM mode behave in the same way. Hence both the modes can be coupled and we reduce the number of equations from 2N to N. Noting the fact that both k and G have only two directions, (-x and +x) or (-y and +y) or (-z and +z) and accordingly we select $\hat{e}_1$ and $\hat{e}_2$. If (-z and +z) is so chosen then $\hat{e}_1$, $\hat{e}_2$ can be set to

$\hat{e}_1 = \vec{x}$, $\hat{e}_2 = \vec{y}$

and the eigen equation can be approximated to a N by N equation group.

$$\sum_{G'} |k+G\|k+G'|\varepsilon^{-1}(\vec{G}-\vec{G}') = \frac{\omega^2}{C^2} h(\vec{G}) \tag{14}$$

Here, D and H are in the x and y plane respectively and TE and TM mode are same.

In case of oblique incidence or in-plane propagation, both K and G are in the same x-y plane, so K+G is also in x-y plane, and one of the unit vectors can be constantly set to: $\hat{e}_{2,k+G} = \hat{z}$ the other unit $\hat{e}_{1,k+G}$ vector is also in the x-y plane. The following leads to some important simplifications:

$$\hat{e}_1 = \langle \cos\theta, \sin\theta, 0 \rangle \text{ and } \hat{e}_2 = \langle 0,0,1 \rangle \tag{15}$$

$$\begin{bmatrix} \hat{e}_2\hat{e}_2' & -\hat{e}_2\hat{e}_1' \\ -\hat{e}_1\hat{e}_2' & \hat{e}_1\hat{e}_1' \end{bmatrix} = \begin{bmatrix} 1 & 0 \\ 0 & \cos(\theta-\theta') \end{bmatrix} \tag{16}$$

i.e., the 2N by 2N equation group is decoupled into two equation groups: the TE and TM.

One group only contains H components along $\hat{e}_1$, no components along $\hat{e}_2 = \hat{z}$, and so is called TM wave. The other group only contains H component along $\hat{e}_2 = \hat{z}$, and E has no component along z which is why it is called the TE wave.

Now the TM mode can be formulated as:

$$\sum_{G'} |k+G\|k+G'|\varepsilon^{-1}(\vec{G}-\vec{G}')h_1(\vec{G}') = \frac{\omega^2}{C^2} h_1(\vec{G}) \tag{17}$$

The TE mode can be formulated as

$$\sum_{G'} |k+G\|k+G'|\varepsilon^{-1}(\vec{G}-\vec{G}')(\hat{e}_1 \bullet \hat{e}_1')h_2(\vec{G}') = \frac{\omega^2}{C^2} h_2(\vec{G}) \tag{18}$$

The equation for the TE mode can be rewritten as:

$$\sum_{G'} |k+G| \bullet |k+G'|\varepsilon^{-1}(\vec{G}-\vec{G}')h_2(\vec{G}') = \frac{\omega^2}{C^2} h_2(\vec{G}) \tag{19}$$

i.e. the two unit vectors are not necessary.

Analysis and Discussion

The band structure of a periodic dielectric structure is given by the k-ω relation. As we know that according to the Bloch's theorem, the relation in a periodic structure is also periodic, so it suffices that it is enough to calculate only the k-points in the so called first Brillouin zone. All other k's outside the first Brillouin zone are the same mode as the k in first Brillouin zone. Making use of the symmetry properties, we only need to calculate the k-ω relation in a zone with no symmetry property called irreducible Brillouin zone.

In the irreducible Brillouin zone given a k point, we will obtain a series of eigen-values, i.e., a set of ω points. On changing the corresponding k points, continuously changed ω points for the same band is what we will get. So usually, we only need to calculate those points on the irreducible Brillouin zone edge i.e. the boundary value, since the other frequencies for those k-points inside the irreducible Brillouin zone will fall inside the band region. In addition to these, the entire band structure of the dielectric periodic array is also plotted.

Moreover it turns out that the bands above and below the photonic bandgap can certainly be distinguished by where the power lies- in the high ε regions or in the low ε regions. It is for this reason that it is convenient to refer to the band above the photonic bandgap as the "air band" and the region below the bandgap as "dielectric band". This is just an analogy to the concept of "conduction band" and "valence band" used in electronic band gap theory.

Using eqns. (17-19), the photonic band structure of a semiconductor heterostructure based photonic crystal is obtained. Fig. 1 and fig. 2 depict the band structure of the crystal within the first Brillouin zone and the band structure of the entire periodic structure respectively for AlGaN/GaN SiO_2/Air material composition under both the TE and TM mode of wave propagation. Similarly, fig. 3 and fig. 4 depict the band structure of the crystal with SiO_2/Air material composition within the first Brillouin zone and the band structure of the entire periodic structure under both the modes of propagation respectively.

Fill factor (*f*) between any two bands can be written as

$$f = \frac{\int_{V\varepsilon 1} \vec{E}^*(\vec{r}).\vec{D}(\vec{r})dv}{\int \vec{E}^*(\vec{r}).\vec{D}(\vec{r})dv} \tag{20}$$

It measures the amount of energy located inside the high dielectric permittivity material.

As seen from fig. 1a, in case of AlGaN/GaN composition under TE mode, the presence of photonic bandgap is prominent in the higher order bands as compared to the lower ones. This is because the filling fraction (*f*) for the TE mode in the lower order bands does not contrast strongly. The *f* computed say, for the first and second band is 0.1 and 0.2 respectively (from eqn. 20). In both these cases we see that they have significant amplitude in the air regions, raising their frequencies. But the field is always trying to be concentrated inside the dielectric to lower their frequency. Due to the absence of continuous pathway in any one of the dielectric, it tends to penetrate inside another. Due to this behavior, neither of the bands is strongly concentrated.

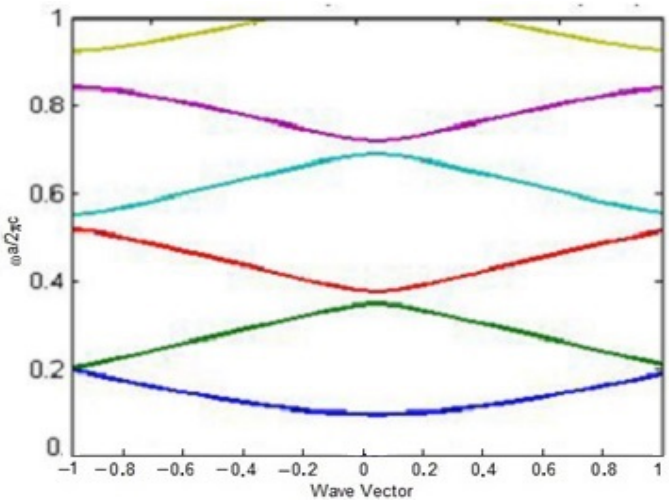

Figure 1a: Band structure of a photonic crystal with AlGaN/GaN composition in first Brillouin zone under TE mode

Since the bands don't contrast each other, hence the large frequency splitting is almost absent, as evident form fig. 1b. However as we go up in the frequency scale, say, for the fifth and sixth bands, we find the value of *f* to be 0.8 and 0.3 (from eqn. 20) respectively. The fifth band has much of its power in the dielectric region and hence possesses low frequency. In comparison, the sixth band has much of its power in the air regions and is associated with high frequency. We find quite a large number of bandgaps occurring in the structure as we move up under TE mode.

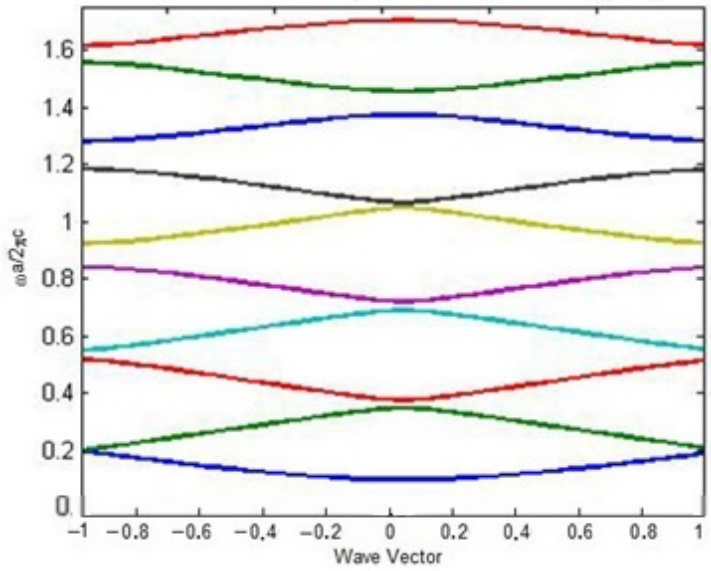

Figure 1b: Complete band structure of a photonic crystal with AlGaN/GaN material composition under TE mode

Fig. 2 gives the plot for the TM mode. Fig. 2a specifically shows the band structure within the first Brillouin zone whereas the complete band structure is depicted in fig. 2b. A prominent and distinguishable bandgap is seen between the fifth and sixth as well as the seventh and eighth bands.

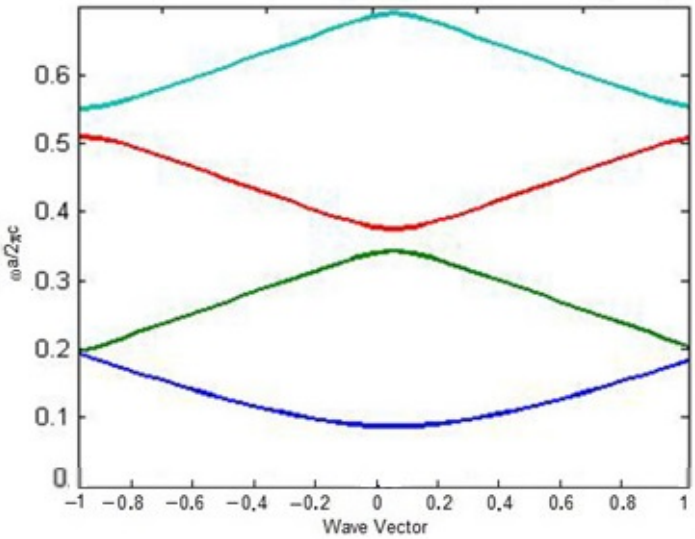

Figure 2a: Band structure of a photonic crystal with AlGaN/GaN material composition in the first Brillouin zone under TM mode

Since mainly the bandgaps are seen to occur in the middle, the reason for this can be can be explained as follows: for TM mode, the displacement field is oriented normal to the plane of propagation, which gives $\vec{D}(\vec{r}).\hat{k} = d(\vec{r})\hat{k}.\hat{k} = d(\vec{r})$. This is a pure scalar function with finite value. For the fifth and sixth as well as the seventh and eighth bands, the fields associated with dielectric material with higher permittivity are strongly concentrated in that region.

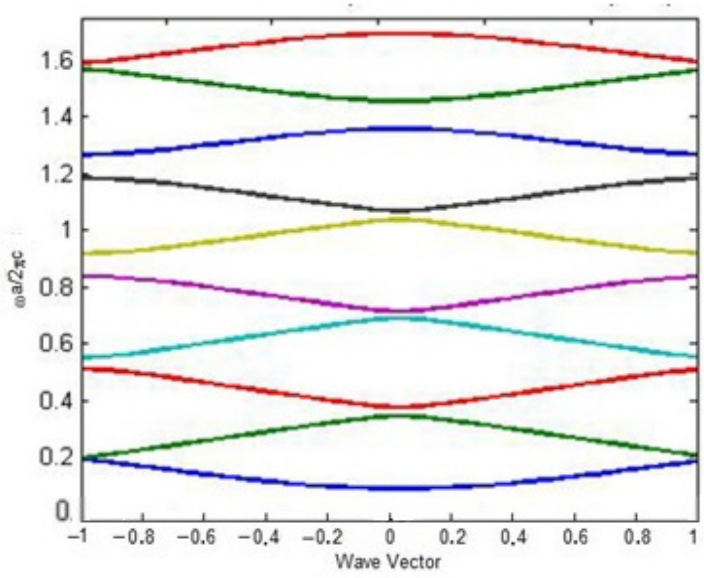

Figure 2b: Complete band structure of a photonic crystal with AlGaN/GaN material composition under TM mode

Hence frequency of light for a given wavelength is lower in that region. The eigen-modes that have most of their characteristics in that region have lower frequency than that of in the other region.

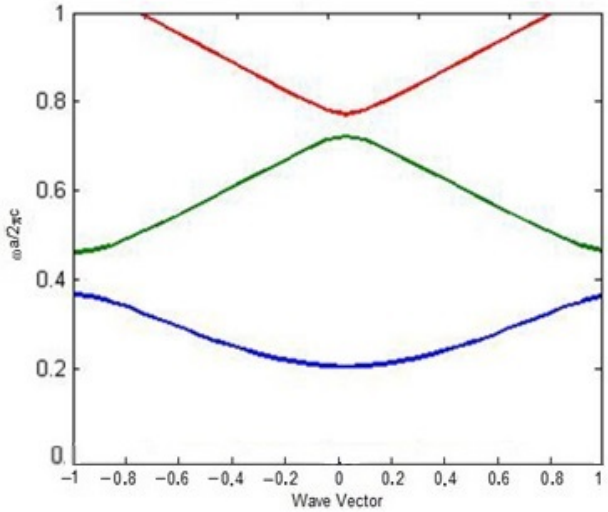

Figure 3a: Band structure of a photonic crystal with SiO_2/Air material composition in first Brillouin zone under TE mode

Separation of frequency can be graphically represented by larger splitting between the bands compared to that for TE mode. Hence fill factor will become large in the region having higher permittivity, and lower for region with lower permittivity. However in case of the first and second

band, the *f* calculated is 0.2 and 0.3 correspondingly (from eqn. 20) which as seen from the previous case of TE mode is the reason for the absence of a photonic bandgap. In fig. 3a, the band structure within the first Brillouin zone is plotted corresponding to which the complete band structure is shown in fig. 3b for TE mode. As seen previously for normal incidence, under TE mode also a photonic bandgap is obtained between the first and second band as seen in fig. 3a. But in this case, the *f* for the first and the second band is 0.2 and 0.5 respectively. Since the contrast in the *f* is not much hence splitting of the bands is not much predominant. As a result a relatively narrow bandgap is obtained. The amount of power in the dielectric region as well as the air region is of comparable amplitude.

It is because of this we find that as we go up the band structure, we do not find the existence of any photonic bandgap in the structure as seen in fig. 3a. A second yet quite an indistinguishable bandgap is noticed between the third and the fourth band. As opposed to which in case of AlGaN/GaN material composition, the presence of photonic bandgaps is predominant under TE mode, which is clearly an inherent advantage.

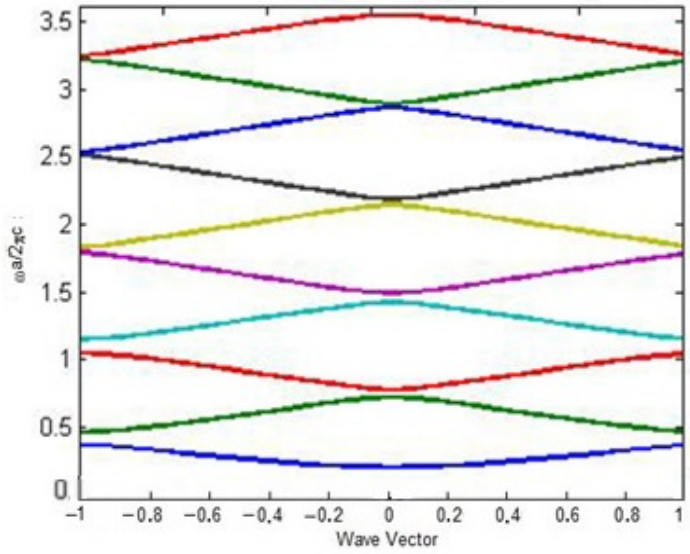

Figure 3b: Complete band structure of a photonic crystal with SiO_2/Air material composition under TE mode

Fig. 4 depicts the band structure of the periodic dielectric array under TM mode. In fig. 4a, apparently it may seem that a similar band structure plot is obtained for the TM mode as was obtained for the TE mode. It is true that the nature of plots in both the cases is quite the same but there is also some difference between the two.

If noticed carefully, we would see that under TM mode also a photonic bandgap is obtained within the first and the second band also. But in this case, for the first band $f = 0.2$ and $f = 0.7$ for the second band (from eqn. 20) and hence, the amount of power conserved by the first band in the dielectric region is formidable as compared to the amount of power saved by the second band in the air region. Hence the difference between the two bands i.e. the first band which is characterized by the low frequency and the second band of high frequency gives rise to a more prominent photonic bandgap in comparison to what was observed for the TE mode.

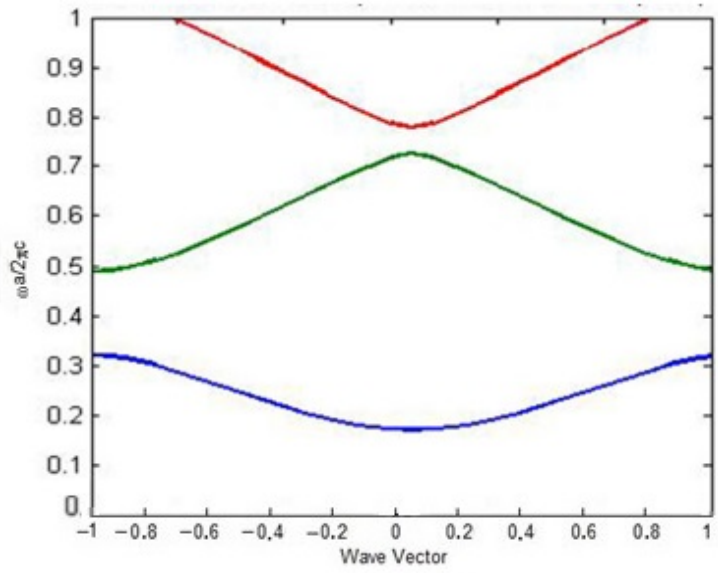

Figure 4a: Band structure of a photonic crystal with SiO_2/Air material composition in the first Brillouin zone under TM mode

One thing to note here is that in case of both TE and TM mode for SiO_2/Air material composition, the *f* factor calculated for the higher order bands are of comparable values which leads them to higher their frequencies. They have no other choice, as the field lines are by nature continuous, hence they are forced to penetrate into the air regions.

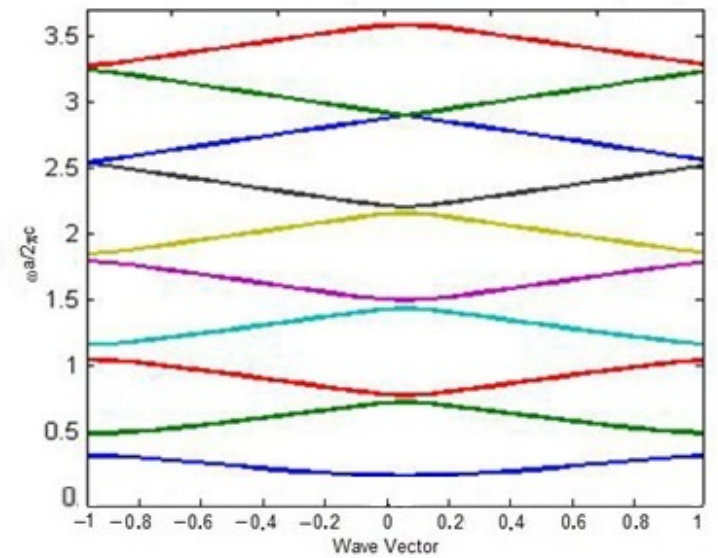

Figure 4b: Complete band structure of a photonic crystal with SiO_2/Air material composition under TM mode

This is actually the reason for the absence of photonic bandgaps in the plots shown. However same is not the case for structures fabricated with AlGaN/GaN which shows a considerable number of photonic bandgaps under both TM and TE mode.

Conclusion

The comparative analysis carried out for both conventional fabricating materials as well as semiconductor heterostructures in fabricating the photonic crystals point out some very important observations which we had plotted and discussed in the earlier sections of this paper. Under oblique incident wave we see the predominance of the number of higher order photonic bandgaps in crystal structures being fabricated with semiconductor heterostructures as compared to its counterpart. Under TE mode of wave incidence, there is a prominent bandgap present only between the first and the second as well as third and fourth band in case of SiO_2/Air material composition in comparison to which bandgaps seem to present between each of the bands from the second band onwards in AlGaN/GaN based composition. The plots for TM mode are no different than the TE mode. Only that here in case of SiO_2/Air composition there is a slight increase in the number of such photonic bandgaps. Such observations testify our claims made in the introductory section of this paper regarding the advantage of the use of semiconductor heterostructure based fabrication in photonic devices in comparison to the traditional material composition under oblique electromagnetic wave.

References

[1] E. Yablonovitch and T. J. Gmitter, "Photonic band structure: The face-centered-cubic case", Phys. Rev. Lett., vol. 63, pp.1950-1953, 1989

[2] R. Loudon, “The Propagation of Electromagnetic Energy through an Absorbing Dielectric”, Journal of Physics A, vol. 3, pp. 233-245, 1970.

[3] D. Mao, Z. Ouyang, and J. C. Wang, “A Photonic-Crystal Polarizer Integrated with the Functions of Narrow Bandpass and Narrow Transmission Angle Filtering”, Applied Physics B, vol. 90, pp. 127-131, 2008.

[4] A. Maity, B. Chottopadhyay, U. Banerjee, and A. Deyasi, “Novel Band-pass Filter Design using Photonic Multiple Quantum Well Structure with P-polarized Incident Wave at 1550 nm”, Journal of Electron Devices, vol. 17, pp. 1400-1405, 2013.

[5] K. Bayat, G. Z. Rafi, G. S. A. Shaker, N. Ranjkesh, S. K. Chaudhuri, and S. Safavi-Naeini, “Photonic-Crystal based Polarization Converter for Terahertz Integrated Circuit”, IEEE Transactions on Microwave Theory and Techniques, vol. 58, pp. 1976-1984, 2010.

[6] R. L. Wang, J. Zhang, and Q. F. Hu, “Simulation of Band Gap Structures of 1D Photonic Crystal”, Journal of the Korean Physical Society, Vol. 52, pp. S71-S74, 2008.

[7] I. S. Fogel, J. M. Bendickson, M. D. Tocci, M. J. Bloemer, M. Scalora, C. M. Bowden, and J. P. Dowling, “Spontaneous Emission and Nonlinear Effects in Photonic Bandgap Materials”, Pure and Applied Optics: Journal of the European Optical Society Part A, vol. 7, pp. 393-408, 1998.

[8] J. C. Chen, H. A. Haus, S. Fan, P. R. Villeneuve, and J. D. Joannopoulos, “Optical Filters from Photonic Band Gap Air Bridges”, Journal of Lightwave Technology, vol. 14, pp. 2575-2580, 1996.

[9] P. Szczepański, “Semiclassical Theory of Multimode Operation of a Distributed Feedback Laser”, IEEE Journal of Quantum Electronics, Vol. 24, pp. 1248-1257, 1988.

[10] J. Hansryd, P. A. Andrekson, M. Westlund, J. Li, and P. O. Hedekvist, “Fiber-based Optical Parametric Amplifiers and their Applications,” IEEE Journal of Selected Topics on Quantum Electronics, vol. 8, pp. 506-520, 2002.

[11] R. Hillebrand, W. Hergert, W. Harm," Theoretical Band Gap Studies of Two-Dimensional Photonic Crystals with Varying Column Roundness", Physica Status Solidi (b), vol. 217, pp. 981-989, 2000.

[12] P. Chhoker, S. Bajaj, "Analysis of Photonic Band Structure in 1-D Photonic Crystal using PWE and FDTD Method", International Journal of Innovative Science, Engineering & Technology, vol. 2, pp. 883-887, 2015

[13] J. Zhao, X. Li, L. Zhong, G. Chen, "Calculation of photonic band-gap of one dimensional photonic crystal "Journal of Physics: Conference Series (Dielectrics 2009: Measurement Analysis and Applications, 40th Anniversary Meeting), vol. 183, p. 012018, 2009.

[14] H. Men, N. C. Nguyenz, R. M. Freundx, P. A. Parrilo, J. Perairek, "Band Gap Optimization of Two-Dimensional Photonic Crystals Using Semidefinite Programming And Subspace Methods" arXiv: 0907.2267 V1 [Math.Oc], 13 Jul 2009.

[15] S. Preble, M. Lipson,"Two-dimensional photonic crystals designed by evolutionary algorithms", Applied Physics Letters, vol. 86, p. 061111, 2005.

[16] C. Y. Kao, S. Osher, E. Yablonovitch, "Maximizing band gaps in two-dimensional photonic crystals by using level set methods", Applied Physics B, vol. 81, pp:235-244, 2005.

[17] Jian-Bo Chen, Yue-Rui Chen, Yan Shen, Wei-Xi Zhou, Jiu-Chun Ren, Yu-Xiang Zheng and Liang-Yao Chen, "Study of the Band-gap Structure of a 1D-photonic Crystal by Using Different Numerical Approaches",Journal of the Korean Physical Society, Vol. 56, No. 4,pp. 1319~1324, 2010.

[18] D.G. Popescu, P.Sterian, "Photonic Crystal Fiber Mode Characterization with Multipole Method", Journal of Advanced Research in Physics, vol. 2, p. 021105, 2011.

[19] D. G. Popescu, "Two Dimensional Photonic Crystals with Different Symmetries for Waveguides and Resonant Cavities Applications", Journal of Advanced Research in Physics, vol. 4, p. 021116, 2013

[20] M. D. Hodge, R. Vetury and J. B. Shealy, "Fundamental failure mechanisms limiting maximum voltage operation in AlGaN/GaN HEMTs", Reliability Physics Symposium (IRPS), 2012 IEEE International, IEEE, (2012).

[21] M. Hadis, "Handbook of Nitride Semiconductors and Devices", GaN-based Optical and Electronic Devices, vol. 3, Wiley.com, (2009).

[22] P. C. Hoang, "Applications of Photonic Crystals in Communications Engineering and Optical Imaging", Diss. Universitätsbibliothek, (2009).